HIGHLIGHTS FROM THE LHCb EXPERIMENT*

Émilie Maurice

on behalf of the LHCb Collaboration

Laboratoire Leprince-Ringuet, CNRS/IN2P3
École Polytechnique, Institut Polytechnique de Paris, Palaiseau, France

Received 25 July 2022, accepted 29 August 2022, published online 14 December 2022

The LHCb experiment has a unique kinematic coverage for heavy-ion physics with its collider and fixed-target configurations. We report on the latest LHCb measurements constraining QCD phenomena.

DOI:10.5506/APhysPolBSupp.16.1-A4

1. Introduction

The LHCb experiment [1] is a single-arm forward spectrometer covering the pseudorapidity (η) range from 2 to 5. It was optimized for the study of hadrons containing b or c quarks. Therefore, LHCb has excellent vertexing, tracking, and particle identification capabilities [2]. On top of that, LHCb provides the unique opportunity for the LHC to operate in a fixed target mode, thanks to the System for Measuring Overlap with Gas (SMOG).

During the LHC Run 2, LHCb collected various proton–nucleus and nucleus–nucleus collisions. In its collider mode, the exploitation of proton–lead (pPb), lead–proton (Pbp), and proton–proton (pp) collisions leads to stringent constraints on hadron production and transport in nuclear environment in high-energy collisions. The lead–lead (PbPb) collisions collected in 2015 and 2018 show the saturation of the LHCb tracking system in the most central collisions (up to 60% centrality). Despite this limitation, the PbPb collisions remain relevant for analyses focusing on ultra-peripheral and peripheral collisions. Complementary to the collider mode, LHCb exploits SMOG to perform physics runs since 2015. Using dedicated LHC fills, LHCb has a unique opportunity to investigate cosmic ray and heavy-ions physics in the high Björken-x region.

* Presented at the 29$^{\rm th}$ International Conference on Ultrarelativistic Nucleus–Nucleus Collisions: Quark Matter 2022, Kraków, Poland, 4–10 April, 2022.

2. Charged and neutral particles production in pPb collisions

LHCb constrains the nuclear PDFs and saturation models at previously unexplored values of the parton momentum fraction, down to $x \sim 10^{-6}$, with the measurements and comparisons of charged and neutral particles production in pPb, Pbp, and pp collisions.

The production of prompt charged particles in pPb and pp collisions is studied at the nucleon–nucleon centre-of-mass energy $\sqrt{s_{NN}} = 5$ TeV as a function of pseudorapidity and transverse momentum (p_{T}) with respect to the proton beam direction [3]. The nuclear modification factor, ratio between the cross section per nucleon in pPb with respect to pp collisions, is determined as a function of η and p_{T} in the backward region ($-4.8 < \eta < -2.5$) and in the forward region ($2.0 < \eta < 4.3$). The results, presented in Fig. 1, show a suppression of charged particle production in pPb collisions relative to pp collisions in the forward region and an enhancement in the backward region for p_{T} larger than 1.5 GeV/c. This measurement highlights a pseudorapidity dependence that nPDF alone cannot describe.

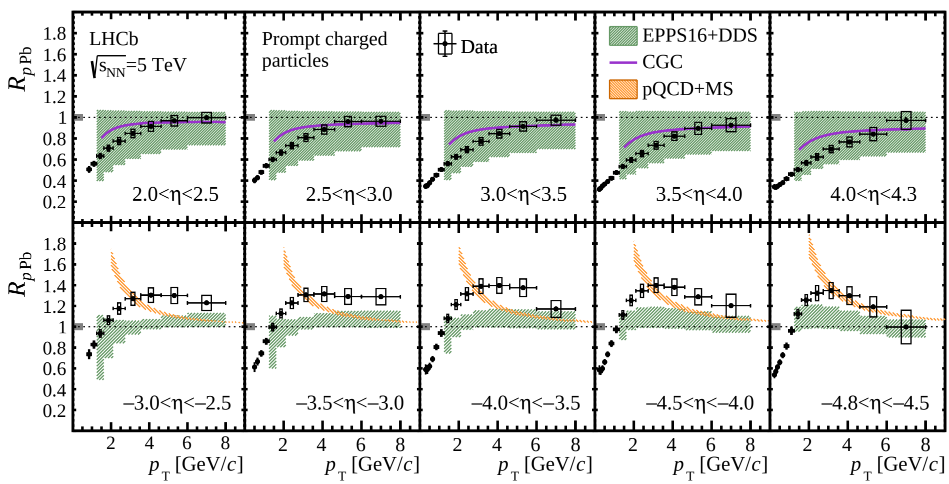

Fig. 1. Nuclear modification factor for prompt charged particles as a function of p_{T} in different η intervals for the (top) forward and (bottom) backward regions in pPb collisions, compared with predictions [3].

The production of neutral pions is measured in pPb collisions collected at a center-of-mass energy per nucleon pair of 8.16 TeV [4]. The π^0 production cross section is measured differentially in the transverse momentum for $1.5 < p_{\mathrm{T}} < 10.0$ GeV and in center-of-mass pseudorapidity (η_{CM}) regions $2.5 < \eta_{\mathrm{CM}} < 3.5$ (forward) and $-4.0 < \eta_{\mathrm{CM}} < -3.0$ (backward) defined relative to the proton beam direction. Results are presented in Fig. 2 and compared to the charged particle production measurements. The forward measurements show a sizable suppression of π^0 production, while the backward measurements show the first evidence of π^0 enhancement in pPb collisions at the LHC.

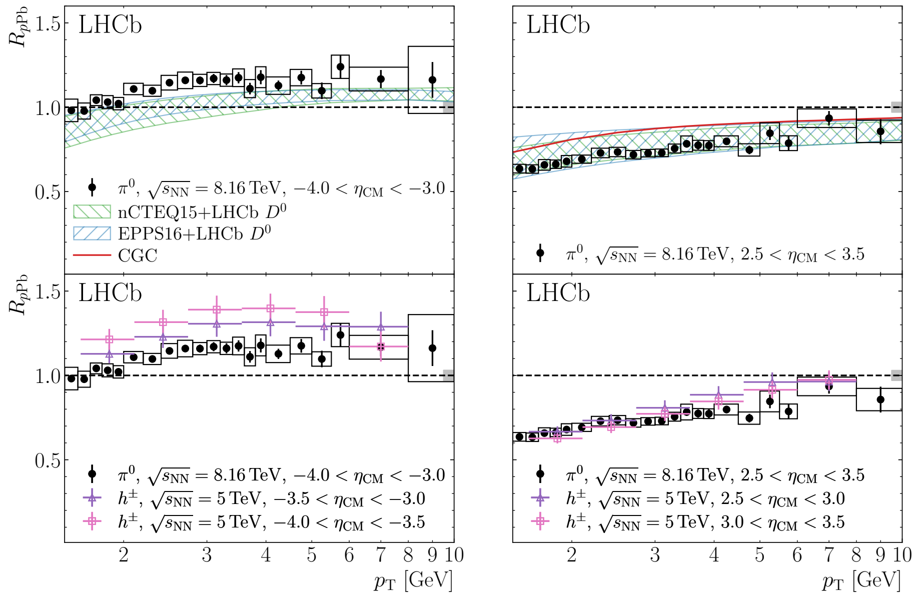

Fig. 2. Measured π^0 nuclear modification factor in the (left) backward and (right) forward η_{CM} regions in pPb collisions [4].

Together, these charged and neutral measurements suggest baryon enhancement in pPb compared to pp collisions. They provide precise constraints on models of nuclear structure and particle production in high-energy nuclear collisions.

3. Exotic hadrons production

The LHCb detector has demonstrated excellent capabilities to discover new particles such as tetraquarks or pentaquarks in pp collisions. LHCb is now investigating the nature of the $X(3872)$ state, also known as $\chi_{c1}(3872)$, but also its capability to probe the QCD medium. More precisely, $\chi_{c1}(3872)$ production in pp and pPb collisions is compared with $\psi(2S)$ production, both decaying into $J/\psi\pi^+\pi^-$ at forward and backward rapidity [5, 6]. Figure 3 suggests that the $\chi_{c1}(3872)$ state experiences different dynamics in the nuclear medium than conventional hadrons. This first measurement of the production of an exotic hadron in pPb collisions provides new constraints on models of $\chi_{c1}(3872)$ structure and models of hadron production and transport in nuclear collisions.

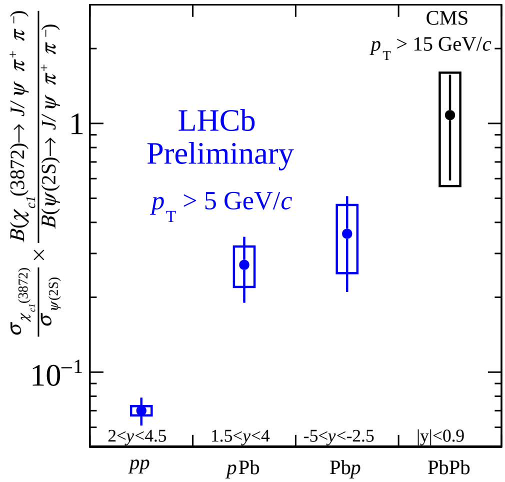

Fig. 3. The ratio of $\chi_{c1}(3872)$ to $\psi(2S)$ cross sections in the $J/\psi\pi^+\pi^-$ decay channel, measured in different collisions [6].

4. Probing QCD with Z^0 boson

Z^0 production measurements are particularly relevant to probe QCD medium. Exploiting *pp* collisions, LHCb has measured for the first time the angular coefficients of the Drell–Yan $\mu^+\mu^-$ pairs in the forward rapidity region [7] and has measured the differential and total Z^0 cross sections at 13 TeV [8] with similar accuracy as the NNLO perturbative QCD predictions. Moreover, the comparison of the LHCb measurement of the fraction of Z^0 + jet events containing a charm jet in intervals of Z^0 rapidity with the NLO calculations at 13 TeV shows a sizable enhancement at forward rapidities, consistent with a proton wave function containing a sizable intrinsic charm component as predicted by LFQCD [9].

Studying the Z^0 production in *p*Pb collisions and comparing it to *pp* measurements is a relevant nPDF test. LHCb has presented the first measurement of the differential Z^0 production cross section in the forward region using *p*Pb collisions, at a nucleon–nucleon centre-of-mass energy of $\sqrt{s_{NN}} = 8.16$ TeV [10]. The forward–backward ratio and the nuclear modification factors are measured together with the differential cross section as functions of the Z^0 rapidity in the centre-of-mass frame and its transverse momentum. The results, presented in Fig. 4, are in good agreement with the predictions from nPDFs, providing strong constraints at small and large Björken-x.

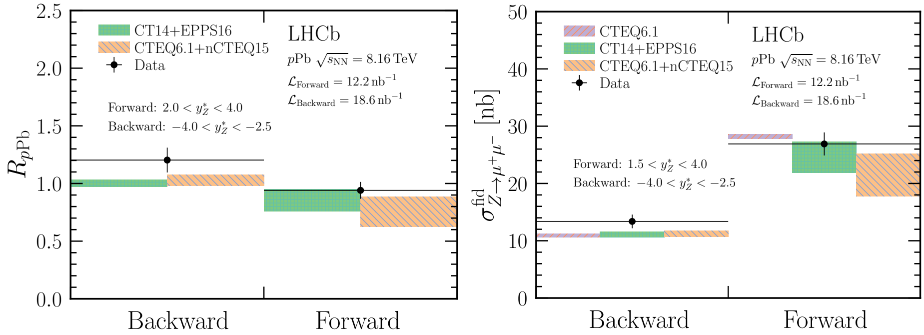

Fig. 4. Measurements of the nuclear modification factor ($R_{p\text{Pb}}$, left) and overall $Z^0 \to \mu^+\mu^-$ production fiducial cross section (right) [10].

5. Heavy flavour production in pPb and PbPb collisions

Heavy-flavour production is a powerful probe of QCD medium, from testing the hadronization process to the investigations of the quark–gluon plasma.

LHCb has recently measured the production of prompt D^0 mesons in pPb collisions at a center-of-mass energy per nucleon pair of $\sqrt{s_{NN}} = 8.16$ TeV, and compared it with measurements in pp collisions [11]. The corresponding nuclear modification factors are determined as a function of the transverse momentum and rapidity in the nucleon–nucleon center-of-mass frame y^*. In the forward-rapidity region, a significant suppression is measured, providing a stringent test of the nPDFs down to the low Björken-x region ($\sim 10^{-6}$). In addition a large asymmetry between the forward and backward production is observed.

LHCb has also investigated the production rate of B^0_s mesons relatively to B^0 mesons, in pp collisions at $\sqrt{s} = 13$ TeV over the forward rapidity interval $2 < y < 4.5$ as a function of the charged particle multiplicity measured in the event [12]. An increase of the ratio B^0_s/B^0 cross sections with multiplicity at transverse momenta below 6 GeV$/c$ is observed at the 3.4σ level, while no significant multiplicity dependence at higher transverse momentum is found as presented in Fig. 5. Comparison with data from e^+e^- collisions implies that the density of the hadronic medium may affect the production rates of B mesons. This is qualitatively consistent with the emergence of quark coalescence as an additional hadronization mechanism in high-multiplicity collisions.

Even if the LHCb tracking system saturates for the most central collisions, the study of ultra-peripheral (UPC) and peripheral collisions is possible and relevant. LHCb has recently published its procedure to determine

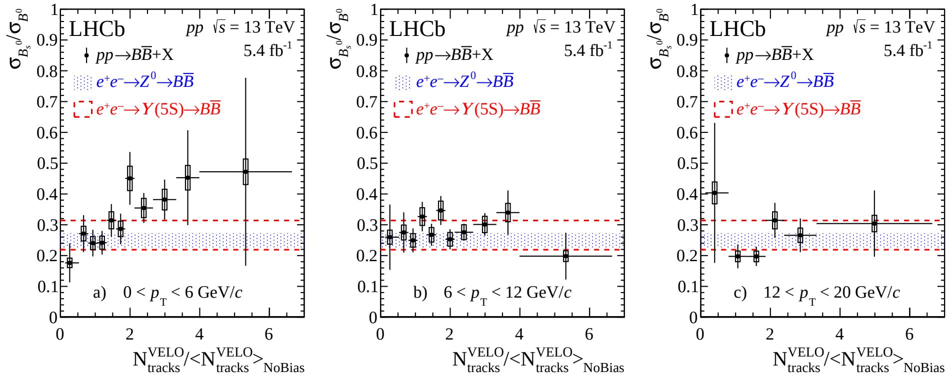

Fig. 5. Ratio of cross sections $\sigma_{B^0_s}/\sigma_{B^0}$ *versus* normalized multiplicity in the transverse momentum ranges (a) $0 < p_{\mathrm{T}}$ <6 GeV/c, (b) $6 < p_{\mathrm{T}} < 12$ GeV/c, and (c) $12 < p_{\mathrm{T}} < 20$ GeV/c [12].

the centrality of the nucleus–nucleus collisions, including PbPb collisions and for the first time measurements for fixed-target collisions at the LHC [13]. First studies of PbPb collisions lead to the precise measurement of the coherent production of J/ψ and $\psi(2S)$ in UPC [14]. In addition, LHCb has published its first PbPb analysis of peripheral collisions, focusing on the photo-production of J/ψ mesons at low transverse momentum at a centre-of-mass energy per nucleon pair of 5 TeV [15]. The photo-produced J/ψ are disentangled from the hadronical process through dimuon p_{T} spectrum fit. The measured yields of the photo-produced J/ψ are higher at mid-rapidity than forward rapidity, and are consistent with being constant with respect to N_{part}, see Fig. 6. LHCb thus confirms the photo-production of J/ψ in PbPb peripheral collisions, with a qualitative agreement between the data and the theoretical predictions while a normalisation discrepancy remains.

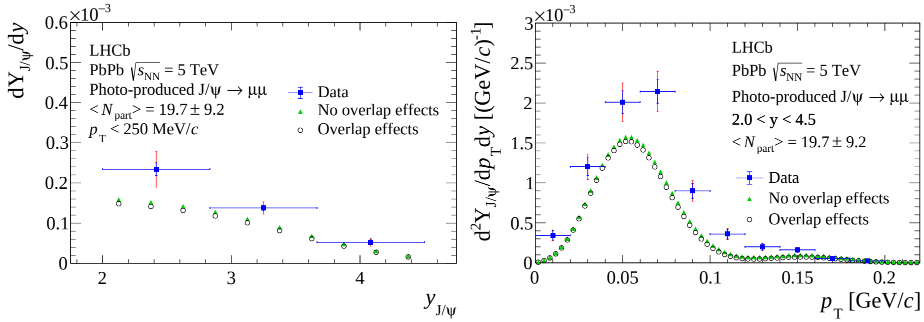

Fig. 6. Differential yields of photo-produced J/ψ candidates as a function of rapidity (left) and transverse momentum (right) [15].

These PbPb peripheral collisions are also studied to measure the production ratio Λ_c^+/D^0 as functions of p_T, y, and $\langle N_{part}\rangle$ [16]. The different dependencies are all consistent with a constant trend around $R(\Lambda_c^+/D^0) \sim 0.27$, consistent with previous LHCb measurements in pPb collisions and compatible within 2σ with PYTHIA 8 prediction in pp collisions including the colour recombination mechanism.

6. Fixed-target program

In addition to the collider configuration, LHCb has the unique possibility, among the LHC experiments, to be operated in fixed target mode, using its internal gas target SMOG. The energy scale achievable at the LHC and the excellent detector capabilities allow a wealth of measurements of great interest for cosmic ray and heavy-ions physics.

After a first publication about charm production in this configuration [17], demonstrating the feasibility of such measurement, LHCb has presented measurements of the J/ψ production in pNe collisions at $\sqrt{s_{NN}} = 68.5$ GeV with the first $\psi(2S)/J/\psi$ ratio [18] and the first analysis of PbNe collisions, collected at the same energy. Testing the $J/\psi/D^0$ production ratio in PbNe as a function of the number of binary collisions shows that additional cold nuclear matter effects affect J/ψ production and that no quark–gluon plasma is created in PbNe collisions at $\sqrt{s_{NN}} = 68.5$ GeV within the current uncertainties [19].

The LHCb cosmic ray program focuses on the interpretation of antiproton flux measurements from space-borne experiments, which is currently limited by the knowledge of the antiproton production cross section in collisions between primary cosmic rays and the interstellar medium. Using pHe collisions at $\sqrt{s_{NN}} = 110$ GeV, LHCb measures the ratio of antiprotons originating from antihyperon decays to prompt production for antiproton momenta between 12 and 110 GeV/c [20]. The antihyperon contributions to antiproton production are observed to be significantly larger than predictions of commonly used hadronic production models.

7. Conclusions

With the LHC Run 2, LHCb has demonstrated strong capabilities to constrain QCD in pp, pPb, and Pbp collisions and promising performances for PbPb collisions and fixed-target physics for the Run 3 and beyond. From 2022, LHCb will benefit from a major upgrade: most of its subdetectors have been replaced and its read-out is fully software-based. Current simulation studies show that no saturation is expected in PbPb collisions up to 30% centrality. In addition, new tracking stations will be installed inside the magnet during the next Long Shutdown, and in ~ 2030 the Mighty Tracker, central part of the tracking system, will be installed, removing the PbPb centrality limitation. Therefore, the LHCb heavy ions physics scope will clearly enlarge in the coming LHC runs.

In addition, the fixed-target program will take full advantage of SMOG2, a 20-cm-long gas storage cell, located upstream of the LHCb nominal interaction point. It allows an increase in the gas pressure (up to a factor 100 compare to SMOG), and also the injection of non-noble gases such as H_2, D_2, O_2 complementary to noble gases up to Xe. Moreover, the decorrelation between the fixed-target and *pp* interaction points offers the opportunity to run simultaneously in both modes. Current studies, with dedicated reconstruction and trigger, demonstrate excellent separation between both interaction points and excellent reconstruction efficiencies, even if upstream of the standard *pp* point. In addition, the first data-driven method fully based on fixed-target data has been published [21], which paves the way to more data-driven techniques thanks to the larger statistics expected with SMOG2. Therefore, with the fixed-target upgrade, LHCb has the unique opportunities to extend its heavy-ion, QCD, and astrophysics program.

REFERENCES

[1] LHCb Collaboration, *J. Instrum* **3**, S08005 (2008).
[2] LHCb Collaboration, *Int. J. Mod. Phys. A* **30**, 1530022 (2015).
[3] LHCb Collaboration, *Phys. Rev. Lett.* **128**, 142004 (2022).
[4] LHCb Collaboration, arXiv:2204.10608 [nucl-ex].
[5] LHCb Collaboration, *Phys. Rev. Lett.* **126**, 092001 (2021).
[6] LHCb Collaboration, CERN-LHCb-CONF-2022-001.
[7] LHCb Collaboration, *Phys. Rev. Lett.* **129**, 091801 (2022), arXiv:2203.01602 [hep-ex].
[8] LHCb Collaboration, *J. High Energy Phys.* **2022**, 026 (2022).
[9] LHCb Collaboration, *Phys. Rev. Lett.* **128**, 082001 (2022).
[10] LHCb Collaboration, arXiv:2205.10213 [hep-ex].
[11] LHCb Collaboration, arXiv:2205.03936 [nucl-ex].
[12] LHCb Collaboration, arXiv:2204.13042 [hep-ex].
[13] LHCb Collaboration, *J. Instrum.* **17**, P05009 (2022).
[14] LHCb Collaboration, arXiv:2206.08221 [hep-ex].
[15] LHCb Collaboration, *Phys. Rev. C.* **105**, L032201 (2022).
[16] LHCb Collaboration, LHCb-PAPER-2022-006, in preparation.
[17] LHCb Collaboration, *Phys. Rev. Lett.* **122**, 132002 (2019).
[18] LHCb Collaboration, LHCb-PAPER-2022-014, in preparation.
[19] LHCb Collaboration, LHCb-PAPER-2022-011, in preparation.
[20] LHCb Collaboration, arXiv:2205.09009 [hep-ex].
[21] LHCb Collaboration, *J. Instrum.* **17**, P02018 (2022).